

## **Optimizing the synthesis of titanium oxide nano-crystallites using low cost organic fuels**

\*Shahid Atiq<sup>1)</sup>, Majid<sup>2)</sup>, Saira Riaz<sup>3)</sup> and Shahzad Naseem<sup>4)</sup>

*Centre of Excellence in Solid State Physics, University of the Punjab,  
Quaid-e-Azam campus, Lahore-54590, Pakistan*

<sup>1)</sup>[satiq.cssp@pu.edu.pk](mailto:satiq.cssp@pu.edu.pk)

### **ABSTRACT**

In the present work, TiO<sub>2</sub> nanoparticles have been prepared by a sol-gel auto-combustion method using titanium tetrachloride as a precursor material, with an aim to get the anatase phase for the photocatalytic applications. Six samples were prepared using three different fuel materials i.e., citric acid, urea and glycine, respectively. First three samples were obtained without thermal treatment and last three samples were obtained by sintering the first three samples at 350 °C, using the same three fuel materials. X-ray diffraction revealed that thermally sintered samples were consisting of pure anatase phase. The dielectric parameters were found to decrease with increase in frequency depicting characteristic oxide behaviour. It has been observed that the sample prepared using urea as a fuel material and subsequently sintered at 350 °C revealed better structural and electrical behaviour characteristic of pure anatase phase of TiO<sub>2</sub>. The morphology was examined by scanning electron microscope and growth of particles was found to be much uniform for the sample obtained by using glycine as fuel material.

### **1. INTRODUCTION**

In the last few decades, human lives are greatly affected by the environmental pollution. There are number of organic and inorganic pollutants present in water and air which have lethal effects on the living beings. These pollutants are discharged from various sources and the bio-degradation of these pollutants is usually very slow. The conventional methods are found to be ineffective and incompatible with environment. Therefore, the photocatalytic treatment using semiconductors is found to be the most attractive mean for the destruction of these pollutants and has become an important research topic in the modern scientific world. In this context, titanium dioxide (TiO<sub>2</sub>) helps the purpose of photocatalysis more than any other semiconductor photocatalyst (Chatterjee D, and Dasgupta, S., 2005; Paola et al., 2008).

Titanium dioxide, also known as titania is focused in many studies due to its unique properties depending upon the phase, chemical composition and microstructure (Yana et al., 2006). TiO<sub>2</sub> is chemically stable, abundant and environmental friendly material

(Huang et al., 2010). It is considered to be one of the most significant semi-conductors of n-type having wide band gap (Tanga et al., 2013). This material exists in three crystalline forms known as anatase, rutile and brookite. The first two phases have tetragonal structure and the third form which is not a famous one has orthorhombic structure. The only stable form of  $\text{TiO}_2$  is rutile and other two phases are metastable and they are readily changed to rutile on heating (Paola et al., 2008). But for the nanoparticles of the  $\text{TiO}_2$ , there is a crossover of the thermodynamic stabilities of the anatase and the rutile phases of the titanium dioxide and the nanoparticles of the anatase titanium dioxide are more stable than the rutile (Lazzeri et al., 2001). It is reported that rutile phase is thermodynamically more stable for the particle sizes above 35 nm while anatase phase is thermodynamically more stable below 11 nm (Bottero et al., 2011). Rutile and anatase phases having tetragonal structure are the more famous forms of the titanium dioxide. These two crystals are made with the chains of distorted  $\text{TiO}_6$  octahedra. Unit cell of the rutile phase has two units of  $\text{TiO}_2$  and titanium atom (Ti) is coordinated with six nearby O-atoms wherein every O-atom is coordinated with three atoms of Ti. Anatase has nearly 9% lower density than the rutile phase and its tetragonal unit cell has four  $\text{TiO}_2$  units. It has the same coordination of the atoms of Ti and O as in rutile but there is more substantial distortion in the octahedra as compared to that of rutile (Lazzeri et al., 2001). Many studies are available regarding the photocatalytic application of the  $\text{TiO}_2$ . Rutile phase is rarely found active for the photo-degradation of pollutants in aqueous solution. Only few studies are available in which the photocatalytic activity of the pure brookite powders is examined. It is generally concluded that the anatase phase suits very well for the photocatalytic applications (Paola et al., 2008). In the recent times, many techniques are being used for the preparation of  $\text{TiO}_2$  nanopowders, which include sol-gel process, hydrothermal process, gas condensation etc. But the solution gel combustion method looks very promising for the preparation of the nanoparticles of the metal oxides. Therefore in the present study, pure anatase  $\text{TiO}_2$  nanoparticles are prepared using  $\text{TiCl}_4$  as a precursor material using sol-gel auto-combustion method in order to study its structural, morphological and frequency dependent dielectric parameters.

## **2. EXPERIMENTAL PROCEDURE**

Sol-gel auto-combustion technique was employed for the preparation of  $\text{TiO}_2$  nanopowders using titanium tetrachloride ( $\text{TiCl}_4$ ) as a precursor material. The use of fuel reagent plays a key role in the establishment of phase purity and crystallinity of the materials in this process. In the present work, three different fuel materials have been employed in order to get well-crystalline  $\text{TiO}_2$  samples having pure anatase phase. The effect of sintering on these samples was also studied carefully. Stoichiometric amounts of analytical grade materials such as  $\text{TiCl}_4$ , citric acid ( $\text{C}_6\text{H}_8\text{O}_7 \cdot \text{H}_2\text{O}$ ), urea ( $\text{CH}_4\text{N}_2\text{O}$ ) and glycine ( $\text{NH}_2\text{CH}_2\text{COOH}$ ) were weighed with precise digital balance. For the first sample, appropriate amounts of  $\text{TiCl}_4$  and citric acid (CA) were added to the deionized water to form a homogeneous solution of 50 mL keeping the  $\text{TiCl}_4$  and CA molar ratio of 1:1.  $\text{TiCl}_4$  was added drop-wise as it is highly reactive to air and water. A magnetic capsule was placed in the beaker and the beaker was positioned on the hotplate. Then the whole arrangement was placed in a fume hood in order to avoid any dangerous

effects of fumes exhausted during the experiment. The temperature of the hotplate was raised gradually and at the same time magnetic stirring was initiated. The solution was continuously stirred and evaporated for 3-4 hours, after which a light greenish yellow gel was formed. This gel was heated at a temperature of nearly 350 °C for few minutes after which the process of combustion was started and within 30 minutes, the combustion was completed giving brownish black homogeneous powders. Then the sample was allowed to cool down at room temperature. Even though this sample was in the powder form but it was grinded with the help of mortar and pestle to get fine powder with homogenous particle size. Now the sample was ready and it was named Sp-1. In the similar way, Sp-2 and Sp-3 were prepared using Urea (U) and Glycine (G) as fuel materials, respectively and the final products obtained after auto-combustion were powders of off-white and black colour, respectively. Sp-4 Sp-5, Sp-6 were prepared by sintering Sp-1, Sp-2 and Sp-3 at a temperature of 350 °C for 4 hours so that we got very pure single phase powders of white colour. The synthesized powders were characterized using, Rigaku D/Max-II A, X-ray diffractometer (XRD) for structural analysis. The diffractometer was operated using  $\text{CuK}\alpha$  radiation having  $\lambda=1.54060 \text{ \AA}$ . Dielectric properties of the samples were determined using 1910 LCR meter. A S-3400N Hitachi EMax scanning electron microscope (SEM) has been used for the microstructural analysis of different samples, prepared by sol-gel auto-combustion technique.

### **3. RESULTS AND DISCUSSION**

Crystal structure of the samples was determined using XRD. The diffraction patterns were obtained at  $2\theta$  values varying between  $20^\circ$  and  $80^\circ$ . Fig. 1 shows the diffraction patterns of the samples, Sp-1, Sp-2 & Sp-3. The patterns were mainly indexed on the basis of the body centred tetragonal type structure with space group  $I41/amd$  and space group number 141, simple tetragonal type structure with space group  $P42/mnm$  and space group number 136 and base centered orthorhombic structure with space group  $Cmcm$  and space group number 63, respectively. The patterns of these samples indicate that the products mainly contain the anatase phase but other impurity phases are also present in small amount as cited from the ICSD Reference codes 00-004-0477, 00-034-0180 and 00-009-0309. Moreover, the peaks of these samples are not sharp enough showing the low crystallinity and less phase homogeneity of the samples.

The XRD patterns of the last three samples Sp-4, Sp-5 and Sp-6, which are prepared by sintering the first three samples (Sp-1, Sp-2 and Sp-3) at 350 °C are shown in the Fig. 2. The pattern of Sp-4 shows that the peaks are sharp enough showing good crystallinity but it still has some percentage of rutile phase alongwith the anatase phase. But the XRD patterns of Sp-5 and Sp-6 indicate that the peaks of these samples are sharp enough, having anatase phase as cited from the ICSD Reference code 00-004-0477. Thus these XRD patterns indicate good crystallinity and phase uniformity of these samples. The results of the Sp-5 sample are the best among present series, as its peaks are the sharpest and also only anatase phase is present in the sample showing the excellent crystallinity and phase uniformity. So, it is concluded that sintering of the samples helps to improve the crystallinity and uniformity of the

samples. Moreover, urea is found to be the most efficient fuel material for the preparation of the anatase TiO<sub>2</sub> nanopowders using sol-gel auto-combustion technique.

The XRD data of Sp-5 and Sp-6 was utilized for calculation of lattice parameters 'a' & 'c' and for the determination of the crystallite size. The unit cell parameters were found to be  $a = 3.7813 \text{ \AA}$  and  $c = 9.71 \text{ \AA}$ . These values of lattice parameters were in close agreement with the values mentioned in the ICDD Reference Code 00-004-0477. The average crystallite size was 7.24 nm as determined by using Scherrer's formula. These XRD results were in agreement with the previous work carried out on TiO<sub>2</sub> nanoparticles by Chou et al.

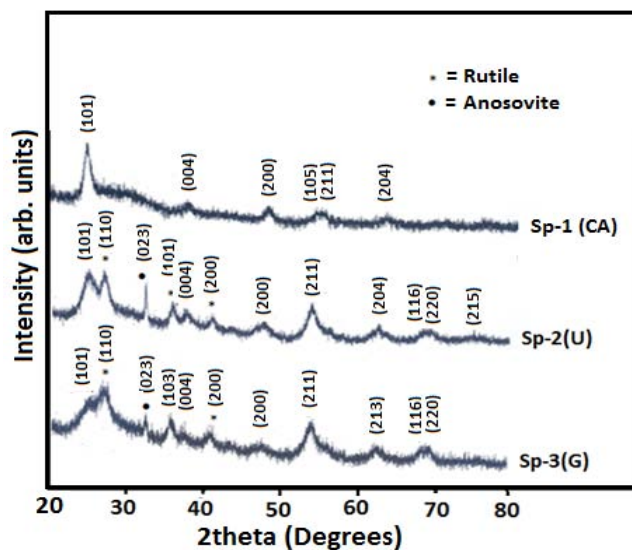


Fig. 1 XRD patterns of samples Sp-1, Sp-2 and Sp-3

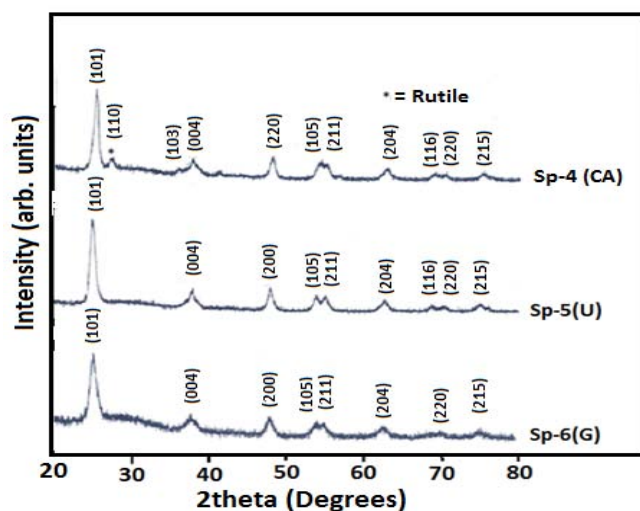


Fig. 2 XRD patterns of samples Sp-4, Sp-5 and Sp-6

Frequency dependent dielectric measurements of Sp-4, Sp-5 and Sp-6 which have been carried out in the frequency range from 1 kHz to 1000 kHz at room temperature are shown in Fig. 3. It is found that the value of dielectric constant ( $\epsilon'$ ) is very high at low frequency and the value of the dielectric constant decreases with increase in frequency for all the samples. It means that the polarization is high at the low frequency giving large value of the dielectric constant. It can be observed that dielectric constant decreases quickly with frequency and then the dielectric constant attains the saturation value at the high frequencies. High value of the dielectric constant at the lower frequencies can be described by space charge polarization because of the inhomogeneous dielectric structure (Lokare et al, 2008). The decrease in the dielectric constant by raising the frequency can be attributed to electrical relaxation processes (Karthik et al., 2010). The net amount of polarization existing in material is because of the ionic, space charge, electronic and dipolar polarizations. This huge value of dielectric constant is because of the fact that  $\text{TiO}_2$  behaves like a nano-dipole under the electric fields. Due to small size of the particles, there are huge number of particles in a unit volume, giving rise to the dipole moment per unit volume, and hence results in high dielectric constant (Sagadevan, 2013). The variation of the dielectric loss ( $\text{Tan}\delta$ ) with frequency shows the similar trend as that of the  $\epsilon'$  as shown in Fig. 4., i.e decrease with increase in frequency.  $\text{Tan}\delta$  is termed as the energy dissipation in the dielectric system, and it is proportional to the imaginary part of dielectric constant (Lokare et al, 2008). In the region of small frequency, energy loss is high and it may be because of the dielectric space-charge, dielectric polarization, and rotation-direction polarization occurring in the region of small frequency (Sagadevan, 2013). Therefore, it is concluded that the variation of  $\epsilon'$  and  $\text{Tan}\delta$  with frequency is almost similar for all the samples which first decreases and then becomes constant.

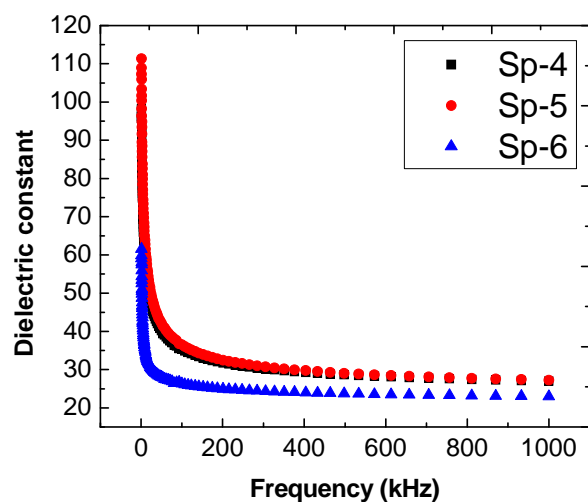


Fig. 3 Frequency dependent dielectric constant of the samples Sp-4, Sp-5 and Sp-6

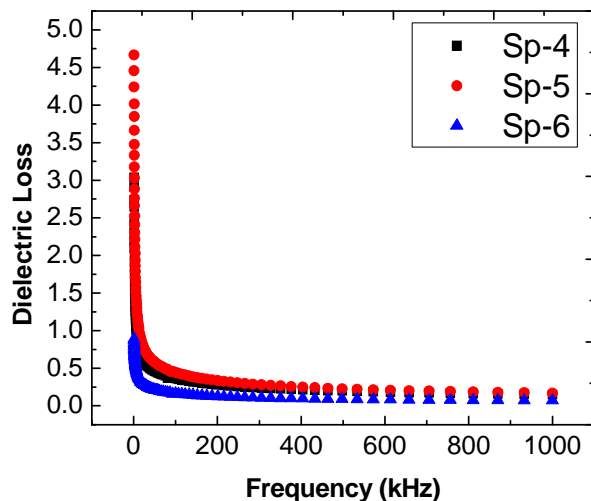


Fig. 4 Frequency dependent dielectric constant of the samples Sp-4, Sp-5 and Sp-6

Microstructural analysis is very useful for the study of structural morphology. Fig. 5 shows the micrographs of the Sp-4, Sp-5 and Sp-6 samples obtained at the same resolution using the samples in the pallets form to study the morphology of the prepared samples. The micrographs reveal that particles are grown in highly densified form. It was observed that the particles were found to be non-uniformly distributed and found either in the clusters of particles or in the form of individually dispersed over the scanned area. The detailed and closer study of these graphs revealed that mostly the

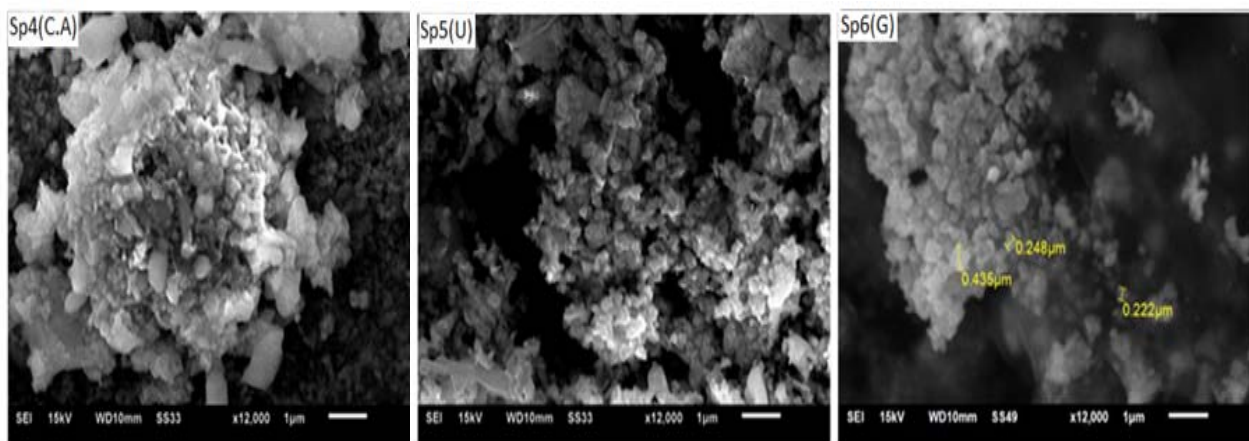


Fig. 5 SEM images of  $\text{TiO}_2$  samples Sp-4, Sp-5 and Sp-6 sintered at 350 °C

particles are almost spherical in form. The agglomeration of particles is weak in Sp-5 and Sp-6 as compared to the Sp-4. The closer inspection of these micrographs discloses a well-defined particle-like morphology, having plenty of spherical particles with the average agglomerated particle size in a range from 0.222  $\mu\text{m}$  to 0.435  $\mu\text{m}$  with average particle size of 0.302  $\mu\text{m}$ . From these images, it is concluded that pure anatase grains are round shaped forming the sponge-like aggregates. Almost similar structural morphology and shape of the particles for the anatase phase has been reported recently by Praveen et al. Preparation condition and the surface chemistry play an important role in the shape stability of the nanoparticles of  $\text{TiO}_2$  (Praveen et al., 2013).

#### 4. CONCLUSIONS

Fuel reagents play a significant role in the preparation of nanoparticles using sol-gel auto-combustion method. In this work, three different organic fuels (citric acid, urea and glycine) have been used to obtain pure anatase  $\text{TiO}_2$ . The phase purity has been confirmed by the XRD analysis. Phase pure anatase nanopowders have been obtained for the samples, Sp-5 and Sp-6, prepared using urea and glycine as fuel agents, respectively, followed by sintering the samples at 350  $^\circ\text{C}$ . Urea has been established as the most appropriate fuel material for preparation of pure anatase phase of  $\text{TiO}_2$ . The average crystallite size, as determined by Scherrer's formula was found to be 7.24 nm. Variation of dielectric constant and dielectric loss as a function of frequency has studied. The values of all these factors first decrease with the increase in frequency and then become constant as the frequency was further increased. The decrease in the values of these parameters is due to electrical relaxation processes. Scanning electron microscope was used to study the surface morphology of the samples in the pallet form. The grains grown in micrometer range were highly densified and their distribution was non-uniform. The spherical shaped particles were mostly found in the form of clusters.

#### REFERENCES

- Bottero, J. Y., Auffan, M., Rose, J., Mouneyrac, C., Botta, C., Labille, J., Masion, A., Thill, A., and Chaneac, C. (2011), "Manufactured metal and metal-oxide nanoparticles: Properties and perturbing mechanism of their biological activity in ecosystems", *C. R. Geosci.*, **343**(2-3), 168-176.
- Chatterjee, D., and Dasgupta, S. (2005), "Visible light induced photocatalytic degradation of organic pollutants", *J. Photoch. Photobio. C*, **6**(2-3), 186–205.
- Chou, C., Guo, M., Liu, K., and Chen, Y. (2012), "Preparation of  $\text{TiO}_2$  particles and their application in the light scattering layer of a dye sensitized solar cell", *Appl. Ener.*, **92**(4), 224-233.
- Huang, B., Chang, F., and Wey, M. (2010), "Photocatalytic properties of redox-treated Pt/ $\text{TiO}_2$  photocatalysts for  $\text{H}_2$  production from an aqueous methanol solution", *Int. J. Hydrogen Energ.*, **35**(15), 7699-7705.

- Karthik, K., Pandian, S. K., and Jaya, N. V. (2010), "Effect of nickel doping on structural, optical and electrical properties of TiO<sub>2</sub> nanoparticles by sol-gel method", *Appl. Surf. Sci.*, **256**(22), 6829–6833.
- Lokare, S. A., Patil, D. R., and Chougule, B. K. (2008), "Structural, dielectric and magnetoelectric effect in (x)BaTiO<sub>3</sub> + (1-x)Ni<sub>0.93</sub>Co<sub>0.02</sub>Mn<sub>0.05</sub>Fe<sub>2</sub>O<sub>4</sub> ME composites", *J. Alloy Compd.*, **453**(1-2), 58–63.
- Lazzeri, M., Vittadini, A., and Selloni, A. (2001), "Structure and energetics of stoichiometric TiO<sub>2</sub> anatase surfaces", *Phys. Rev. B*, **63**, 155409.
- Paola, A. D., Cufalo, G., Addamo, M., Bellardita, M., Campostrini, R., Ischia, M., Ceccato, R., and Palmisano, L. (2008), "Photocatalytic activity of nanocrystalline TiO<sub>2</sub> powders prepared by thermolysis of TiCl<sub>4</sub> in aqueous solutions", *Colloid. Surface A*, **317**(1-3), 366-376.
- Praveen, P., Viruthagiri, G., Mugundan, S., and Shanmugam, N. (2013), "Structural, optical and morphological analyses of pristine titanium di-oxide nanoparticles", *Spectrochim. Acta A*, **117**(1), 622–629.
- Sagadevan, S. (2013), "Synthesis and electrical properties of TiO<sub>2</sub> nanoparticles using a wet chemical technique", *J. Nanosci. Nanotechnol.*, **1**(1), 27-30.
- Tanga, G., Liua, S., Tang, H., Zhang, D., Li, C., and Yang, X. (2013), "Template-assisted hydrothermal synthesis and photocatalytic activity of novel TiO<sub>2</sub> hollow nanostructures", *Ceram. Int.*, **39**(5), 4969–4974.
- Yana, Q., Su, X., Huang, Z., and Ge, C. C. (2006), "Sol-gel auto-igniting synthesis and structural property of cerium-doped titanium dioxide nanosized powders", *J. Eur. Ceram. Soc.*, **26**(6), 915–921.